NONLINEAR FEM ANALYSIS OF THIN-WALLED STEEL TUBULAR COLUMNS WITH IN-FILLED CONCRETE UNDER CYCLIC LOAD

○Ghosh Prosenjit Kumar Student Member Nagoya Institute of Technology
Yoshiaki GOTO Fellow Member Nagoya Institute of Technology

1. Introduction: Partially concrete-filled thin-walled steel tubular columns referred hereinafter as PCFT columns are often preferred as elevated highway bridge piers in Japan due to high earthquake resistance. In PCFT columns, concrete is filled only at the lower part of the hollow columns and confined by diaphragms to reduce the inertia force during earthquake, and the cyclic local buckling of steel tube is restrained due to steel-concrete interaction. There are several cyclic loading experiments to study the hysteretic behavior of PCFT columns. However, up to the present, no sufficient research has been conducted on numerical computation of the hysteretic behavior of PCFT columns in a direct manner. Herein, considering geometric and material nonlinearity, we propose an accurate and numerically stable FEM model that computes the hysteretic behavior of PCFT columns in a direct and versatile manner. Then, the accuracy of the computed results is confirmed by comparing with the results of unidirectional cyclic loading experiment.

2. Typical hysteretic curve of PCFT column: According to unidirectional cyclic loading test results[1)], PCFT columns exhibit a characteristic pinching hysteretic loop shown in **Fig.1**. This typical hysteretic behavior has two distinct features. First, when the horizontal displacement approaches zero, the cracks open due to the decrease of the compressive stress and thereby, stiffness is decreased. However, when the horizontal displacement increases from zero in the opposite direction, the cracks again close on the compressive side and the column recovers its stiffness. Second, being different from hollow or RC columns, the energy dissipation capacity of the hysteretic loop is rather stable due to the restraint of local buckling by the in-filled concrete as well as the confinement of the concrete. Herein, a FEM model is proposed to express the above hysteretic behavior of PCFT columns accurately.

3. Material and interface modeling: Hysteretic behavior of PCFT columns is strongly influenced by the cyclic behavior of the hollow steel tube. Herein, the modified 3-surface cyclic plasticity model[2)] is used as a constitutive model for steel and is implemented in shell element by user subroutine. Regarding the in-filled concrete, material nonlinear behavior is expressed by the concrete damaged plasticity model[3)] implemented in ABAQUS[4)]. This model is more approximate than the conventional plasticity model combined with the smeared cracking model but ensures better numerical stability when applied in FEM model. For the cyclic interface action between tubular column and in-filled concrete, contact model with friction effect in tangential direction is considered. In this model, $\mu = 0.2$ is used as interface friction parameter.

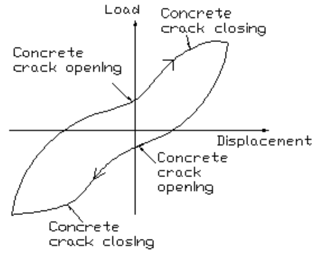

Fig.1 Hysteretic curve of PCFT column with pinching behavior

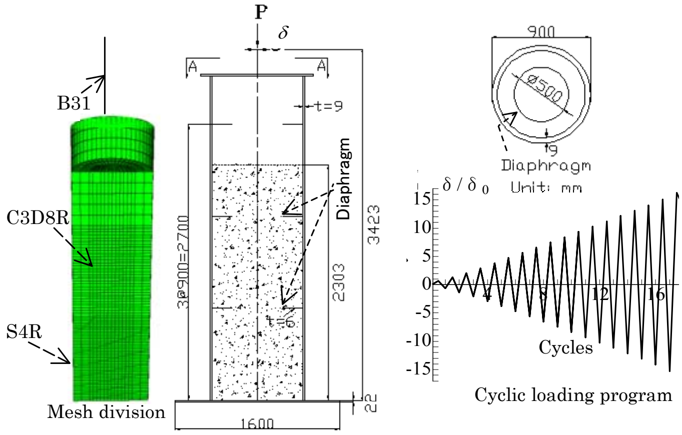

Fig.2 Specimen and analytical model

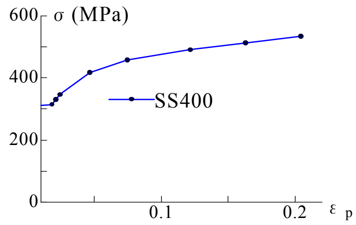

Fig.3 Uniaxial stress-strain relation of steel

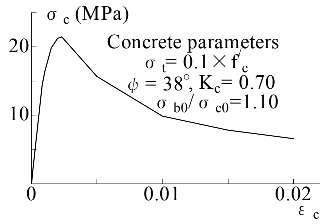

Fig.4 Concrete uniaxial test results

Table 1 Geometric properties of the specimens

Specimens	Height h (m)	Concrete Height (m)	Thicknees, t (mm)	Radius, R(mm)	$\bar{\lambda}$	R_t	δ_0 (mm)	H_0 (kN)	$\frac{P}{\sigma_y A}$
Hollow (No.29)	3.423	--------	9.0	450	0.267	0.123	10.5	400.82	0.199
PCFT (No.30)		2.303							

Key words: Local buckling, hysteretic behavior, FEM analysis, ductility, PCFT column
Contact address: Gokiso-cho, Showa-ku, Nagoya, 466-8555, Japan. (Tel: 052-732-211)

Table 2 3-Surface model parameters

Steel	E_s (GPa)	υ_s	σ_y (MPa)	σ_u (MPa)	ε_{yp}	β	ρ	κ	ξ	f_b/σ_y
SS400	205.8	0.3	308	534	0.0183	150	2	2	0.1	0.25

4. Numerical examples: A PCFT column model for the present analysis illustrated in **Fig.2** is determined based on the PCFT column specimen used in the unidirectional cyclic loading experiment[1]. The geometric parameters for the specimens are summarized in **Table 1**. No.30 and No.29 are PCFT and corresponding hollow columns, respectively. The experimental results of No.29 are used to identify the steel material parameters (**Table 2**) for the 3-surface model. The uniaxial stress-strain relation for the material steel is illustrated in **Fig.3**. Regarding the in-filled concrete, the uniaxial stress-strain relation under compression and the values of the material parameters $\psi, K_c, \sigma_{b0}/\sigma_{co}$, respectively shown in **Fig.4** are used to define constitutive model. These parameters including tensile strength of concrete σ_t are calibrated by using the experimental results of PCFT column so that the numerical results best fit the test results. In the FEM model, the lower part of the steel tube with diaphragms is modeled with the 4-node thick shell element (S4R), while the upper part is modeled by elastic beam element (B31). The concrete core is represented by 8-node solid element (C3D8R). The interaction between the concrete and the steel tube including diaphragms as well as base plate is expressed by contact with friction model explained in section **3.** A geometrically and materially nonlinear numerical analysis is carried out by ABAQUS.

5. Hysteretic behavior of PCFT and hollow columns: The results of unidirectional cyclic loading tests on PCFT (No.30) and hollow (No.29) columns are compared with the computed results of the FEM model in **Figs.5**, in terms of the horizontal restoring force-displacement relation. It can be seen that the accuracy of the FEM model is generally acceptable. Specifically, the computed results rather accurately exhibit the pinching hysteretic loops observed in the experiments of PCFT columns. To examine the effect of the in-filled concrete, the deformed shapes at $\delta = +6.0\delta_0$ and the dissipated energy-horizontal restoring force relations are further shown for PCFT and hollow columns in **Figs.6～7**, respectively. In **Fig.7**, the plastic energy dissipated by the column is approximately calculated by $A_E = \int H d\delta$, where horizontal restoring force $|H| = ABS(H)$ and A_{E0} is an elastic energy given by $A_{E0} = 0.5H_0\delta_0$. From **Figs.5～7**, it can be seen that the strength, ductility and energy dissipation capacity of PCFT columns are significantly improved from those of the hollow columns. This is primarily due to the fact that the local buckling of the steel tube is restrained by the interface action and dilation of in-filled concrete, as shown in **Fig.6**.

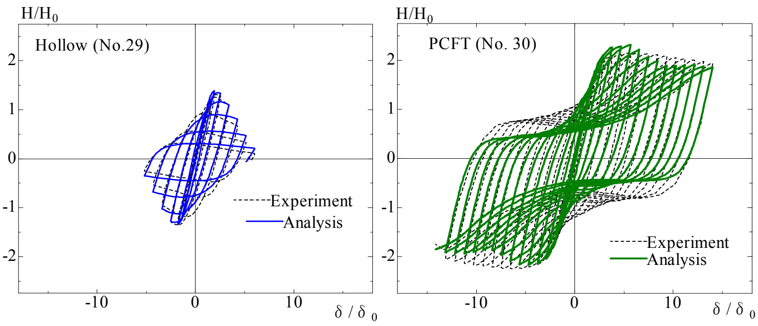

Fig.5 Hysteretic behaviors of hollow and PCFT columns under cyclic load

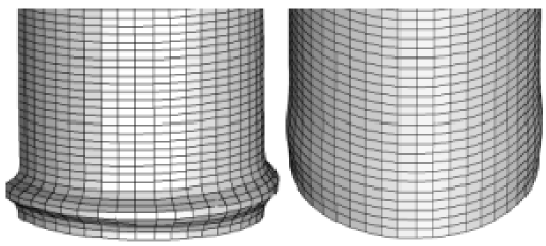

at $\delta = +6.0\delta_0$

(a) Hollow (No. 29) (b) PCFT (No.30)

Fig. 6 Deformed shapes at the lower part of steel pipe (× 1.5)

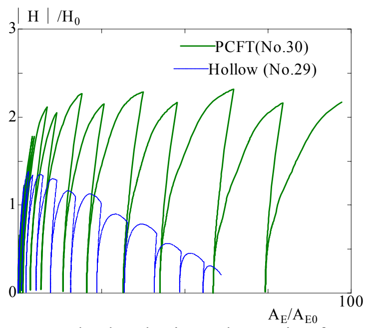

Fig.7 Dissipated energy-absolute horizontal restoring force relation up to $\delta = +6.0\delta_0$

6. Summary and concluding remarks: In view of the practical application to the seismic performance evaluation, an accurate and numerically stable FEM model is proposed to compute the hysteretic behavior of PCFT columns. In this model, 3-surface cyclic plasticity model for steel tube and concrete damaged plasticity model for in-filled concrete are used as constitutive relations. Contact with friction effect is considered for interface modeling. From this computation, it can be concluded that the proposed FEM model for PCFT columns under cyclic load exhibits the pinching hysteretic loop characteristics and the computed results coincide well with the experimental results.

References

1) Public Work Research Institute: Report of cooperative research on limit state seismic design for bridge piers I-VIII and summary, 1997-2000.
2) Goto, Y., Jiang, K. & Obata, M.: Stability and Ductility of Thin-Walled Circular Steel Columns under Cyclic Bidirectional Loading, J. Struct. Eng., ASCE, 132(10): 1621-1631. 2006.
3) Lee, J., & Fenves, G. L.: Plastic-Damage Model for Cyclic Loading of Concrete Structures, Journal of Engineering Mechanics, ASCE, 124(8): 892–900, 1998.
4) ABAQUS/Standard User's Manual, Version 6.6, Hibbit, Karlson &Sorensen, Inc, 2006.